Electronic Supplementary Material (ESI) for Dalton Transactions.
This journal is © The Royal Society of Chemistry 2019

Electronic Supporting Information

for

Lithium cations in a self-assembled electrostatic nanocapsule

Júlia Mayans, Mercé Font-Bardia and Albert Escuer,*

Contents

1.Synthetic details.

$(Et_3NH)_2\{Li(H_2O)\ [Ni_6(CO_3)(N_3)_6(Pz)_3(py_2C(O)(OH))_3]\}_2$. 1.0 mmols (0.365 g) of $Ni(ClO_4)_2\cdot 6H_2O$ was solved in 15 mL of acetonitrile. To this solution were added 0.5 mmol (0.092 g) of dipyridylketone, 0.75 mmol (0.051 g) of pyrazole and 1.5 mmol (0.100 g) of trimethylamine. Finally, 0.75 mmol (0.200 g) of tetrabuthylammonium azide and 0.5 mmol (0.060 g) of lithium perchlorate were added to obtain a clean blue solution that was maintained with vigorous stirring for half hour to incorporate carbon dioxide from the ambient. This solution was left to slow evaporation filtering the reddish precipitate that forms in one-two days. Well-formed blue crystals were obtained after a few days in a 50% yield. Anal. calculated/found (%) for the complex formula: **1**, C, 36.71/37.2; H 3.44/3.3; N 27.09/26.8.

Previous works suggested that the dpk/azide mix of ligands in the presence of carbonate anions and Ni^{II} cations is prone to produce hexanuclear metallocycles. In our case we employed a defect of dpk and adding pyrazole to cover the vacant coordination sites of the Ni^{II} cations. The choice of pyrazole was made on basis of the adequate bite of the ligand and the minus charge that possesses after deprotonation. To reach the lithium complex it was necessary to avoid the presence of other cations that could compete for the coordination sites provided by the O-donors. To this end and to dispose of a high solubility in organic solvents the choice was the employment of the highly soluble tetrabuthylammonium azide. This reagent is not common in cluster chemistry but offers the possibility to obtain new systems that has been restricted until now by the insolubility of sodium azido in solvents different to water or methanol.

Following the same strategy, a complete family of supramolecular capsules and bowls can be obtained varying the size of the alkaline cations or the employed bases. The full description of the reactivity of this system as function of the cation size, cation charge and the organic cation will be described in a further full paper.

The spectra of complex **1** is representative of the systems containing the hexanuclear $[Ni_6(\mu_6\text{-}CO_3)(N_3)_6(pz)_3\{py_2C(O)(OH)\}_3]^{2-}$ metallomacrocycle, being complicated below 1500 cm^{-1} but showing the OH, aliphatic and aromatic C-H stretchings (3400, 3075, 2980-2935 cm^{-1}), the strong azido stretching centered at 2060 cm^{-1} and the set of peaks around 1600 cm^{-1} attributed to the pyrazole ligand.

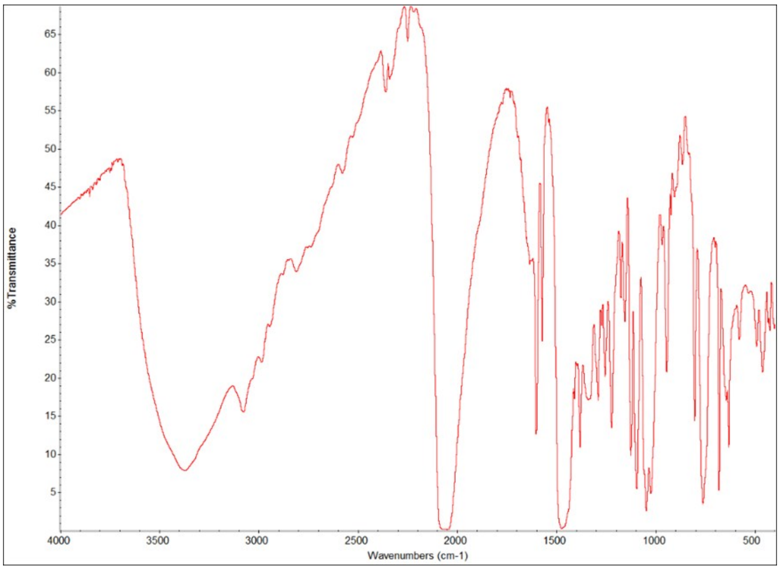

Fig. S1. IR spectrum of complex **1**.

2. Crystal Structure of 1.

Structure determination: A green prism-like specimen of $C_{49}H_{54.75}LiN_{31}Ni_6O_{10.38}$, approximate dimensions 0.112 mm x 0.120 mm x 0.129 mm, was used for the X-ray crystallographic analysis. The X-ray intensity data were measured on a D8 Venture system with a multilayer monochromator and a Mo microfocus (λ = 0.71073 Å).

The frames were integrated with the Bruker SAINT software package using a narrow-frame algorithm. The integration of the data using a triclinic unit cell yielded a total of 166980 reflections to a maximum θ angle of 26.67° (0.79 Å resolution), of which 29179 were independent (average redundancy 5.723, completeness = 98.0%, R_{int} = 10.67%, R_{sig} = 7.20%) and 17728 (60.76%) were greater than $2\sigma(F^2)$. The final cell constants of $\underline{a}$ = 16.9870(9)Å, $\underline{b}$ = 18.1041(9) Å, $\underline{c}$ = 23.7797(12) Å, α = 95.640(2)°, β = 99.050(2)°, γ = 99.754(2)°, volume = 7058.8(6) Å^3, are based upon the refinement of the XYZ-centroids of reflections above 20 σ(I). Data were corrected for absorption effects using the Multi-Scan method (SADABS). The calculated minimum and maximum transmission coefficients (based on crystal size) are 0.6772 and 0.7454.

The structure was solved and refined using the Bruker SHELXTL Software Package, using the space group P -1, with Z = 4 for the formula unit, $C_{49}H_{54.75}LiN_{31}Ni_6O_{10.38}$. The final anisotropic full-matrix least-squares refinement on F^2 with 1761 variables converged at R1 = 5.77%, for the observed data and wR2 = 18.46% for all data. The goodness-of-fit was 1.031. The largest peak in the final difference electron density synthesis was 1.796e^-/Å^3 and the largest hole was -2.297 e^-/Å^3 with an RMS deviation of 0.108 e^-/Å^3. On the basis of the final model, the calculated density was 1.509 g/cm^3 and F(000), 3279 e^-.

Table S1. Crystal and structure refinement data for **1.**

Formula	C49 H54.75 Li N31 Ni6 O10.38
FW	1603.18
System	triclinic
Space group	*P*-1
a/Å	16.9870(9)
b/Å	18.1041(9)
c/Å	23.780(1)
α/deg.	95.640(2)
β/deg.	99.050(2)
γ/deg.	99.754(2)
V/ Å^3	7058.8(6)
Z	4
T, K	303(2)
λ(MoKα), Å	0.71073
ρcalc, g·cm-3	1.509
μ(MoK$_\alpha$), mm^{-1}	1.641
R	0.0577
ωR^2	0.1542

Table S2. Selected distances (Å) and angles (º) for the core of complex **1**.

Ni-O (Carbonate)		**Ni-O (dpk)**	
Ni(1)-O(7)	2.080(3)	Ni(1)-O(1)	2.096(4)
Ni(2)-O(8)	2.074(3)	Ni(2)-O(1)	2.101(4)
Ni(3)-O(8)	2.078(4)	Ni(3)-O(3)	2.078(4)
Ni(4)-O(9)	2.086(4)	Ni(4)-O(3)	2.053(4)
Ni(5)-O(9)	2.074(3)	Ni(5)-O(5)	2.057(4)
Ni(6)-O(7)	2.078(4)	Ni(6)-O(5)	2.051(4)
Ni-N (azide)			
Ni(1)-N(13)	2.085(5)	Ni(4)-N(22)	2.162(5)
Ni(2)-N(13)	2.100(5)	Ni(5)-N(22)	2.161(5)
Ni(2)-N(16)	2.157(5)	Ni(5)-N(25)	2.083(5)
Ni(3)-N(16)	2.176(5)	Ni(6)-N(25)	2.100(5)
Ni(3)-N(19)	2.096(5)	Ni(6)-N(28)	2.189(5)
Ni(4)-N(19)	2.092(5)	Ni(1)-N(28)	2.149(5)
Ni- (pyrazole)		**Ni···Ni**	
Ni(1)-N(12)	2.033(5)	Ni(1)···Ni(2)	2.997(1)
Ni(2)-N(3)	2.050(5)	Ni(2)···Ni(3)	3.089(1)
Ni(3)-N(4)	2.026(5)	Ni(3)···Ni(4)	3.0155(9)
Ni(4)-N(7)	2.030(5)	Ni(4)···Ni(5)	3.0635(9)
Ni(5)-N(8)	2.025(5)	Ni(5)···Ni(6)	2.999(1)
Ni(6)-N(11)	2.012(5)	Ni(6)···Ni(1)	3.0685(9)
Ni(1)-N(13)-Ni(2)	91.5(2)	Ni(1)-O(1)-Ni(2)	91.1(1)
Ni(2)-N(16)-Ni(3)	91.0(2)	Ni(3)-O(3)-Ni(4)	93.8(2)
Ni(3)-Ni(19)-Ni(4)	92.1(2)	Ni(5)-O(5)-Ni(6)	93.8(1)
Ni(4)-N(22)-Ni(5)	90.3(2)	Ni(2)-O(8)-Ni(3)	96.2(1)
Ni(5)-N(25)-Ni(6)	91.6(2)	Ni(4)-O(9)-Ni(5)	94.9(1)
Ni(6)-N(28)-Ni(1)	90.0(2)	Ni(6)-O(7)-Ni(1)	95.1(1)

3. Magnetic properties of 1.

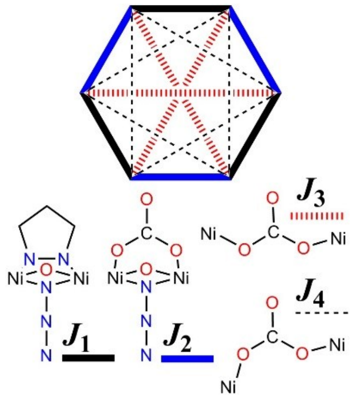

Fig. S2. Coupling scheme of the superexchange interactions for the hexanuclear metallomacrocycle.

The {Ni_6} ring has four different superexchange pathways, two of them involving the azido ligands as part of a triple bridge and two of them involving the only the carbonato ligand. In basis on the structural data the complete Hamiltonian is:

$$H = -2J_1(S_1\cdot S_2 + S_3\cdot S_4 + S_5\cdot S_6) -2J_2(S_2\cdot S_3 + S_4\cdot S_5 + S_1\cdot S_6) -2J_3(S_1\cdot S_3 + S_1\cdot S_5 + S_2\cdot S_4 + S_2\cdot S_6 + S_3\cdot S_5 + S_4\cdot S_6) -2J_4(S_1\cdot S_4 + S_2\cdot S_5 + S_3\cdot S_6)$$

The main interactions that determine the magnetic response of **1** should be J_1 and J_2 because the *syn-anti* and *anti-anti* pathways related exclusively to the carbonato bridge are poor mediator between paramagnetic centres.

Fit of the experimental data yield the coupling constant values: J_1 = -6.9 cm^{-1}, J_2 = -11.0 cm^{-1}, J_3 = -0.7 cm^{-1}, J_4 = 2.6 cm^{-1}, g = 2.15, $R = 1.5\cdot 10^{-5}$. (R quality factor defined as $(\chi_M T_{exp}-\chi_M T_{calc})^2/(\chi_M T_{exp})^2$). By comparison with the related derivatives with dypyridyl-diol (reference 8, main text), the antiferromagnetic interaction parametrized as J_1 must be assigned to the superexchange pathway participated by the pyrazole bridge.

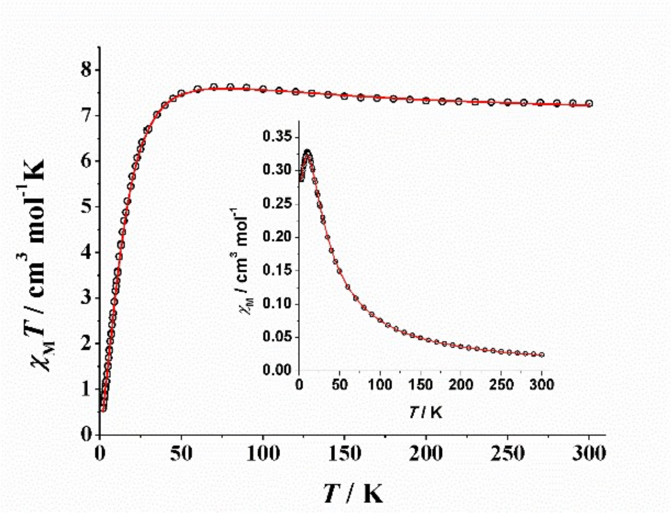

Fig. S3. $\chi_M T$ vs. T plot for complex **1**. Inset, χ_M vs. T plot showing the maximum of susceptibility that determines the $S = 0$ ground state.